



**Univerzita Komenského v Bratislave**  
**Fakulta matematiky, fyziky a informatiky**



**RNDr. Andrej Vojtko**

**Autoreferát dizertačnej práce**

**Nanoparticles and Nanoparticle Assemblies for Advanced Photovoltaic Organic Structures**

**na získanie akademického titulu philosophiae doctor**

**v odbore doktorandského štúdia:**

**Fyzika kondenzovaných látok a akustika**

**Bratislava 7.6.2016**

**Dizertačná práca bola vypracovaná**

v dennej forme doktorandského štúdia

**na Fyzikálnom ústave Slovenskej Akadémie Vied**

**Predkladateľ:**            **RNDr. Andrej Vojtko**  
Fyzikálny ústav SAV  
Dúbravská cesta 9  
845 11 Bratislava

**Školiteľ:**                 **RNDr. Eva Majková, DrSc.**  
Fyzikálny ústav SAV

**Oponenti:**                 .....

.....

.....

.....

.....

.....

**Obhajoba dizertačnej práce sa koná ..... o ..... h**  
**pred komisiou pre obhajobu dizertačnej práce v odbore doktorandského štúdia vymenovanou**  
**predsedom odborovej komisie .....**

**Fyzika kondenzovaných látok a akustika**

**na**

.....

**Predseda odborovej komisie:**  
**Prof. RNDr. Peter Kúš, DrSc.**  
Fakulta matematiky, fyziky a informatiky UK  
Mlynská dolina F1  
842 48 Bratislava

## Abstrakt

Táto práca pojednáva najmä o zabudovaní rôznych druhov nanočastíc do organických fotovoltických štruktúr za účelom zvýšenia ich účinnosti. Hlavná časť práca je venovaná použitiu plazmonických nanočastíc v organických solárnych článkoch na báze zmesi P3HT:PCBM. Do aktívnej vrstvy boli zabudované tri typy plazmonických nanočastíc: chemicky syntetizované strieborné a zlaté nanočastice a zlaté nanočastice pripravené metódou laserovej ablácie terčika v kvapaline. Pre chemicky syntetizované nanočastice obalené surfaktantom boli pozorované zlepšenia prúdovej hustoty nakrátko, zlepšenie spôsobili viaceré mechanizmy. Ako možný dôvod bola označená rozdielnosť surfaktantov. Pre zlaté nanočastice sme pozorovali plazmonické zlepšenie prúdovej hustoty nakrátko, ale plniaci faktor bol výrazne zhoršený. Strieborné nanočastice vykázali 10%-né zlepšenie účinnosti článku, ale plazmonický efekt na zlepšenie prúdu nakrátko nebol pozorovaný. Použitím bezsurfaktantových nanočastíc sme sa vyhli vplyvu surfaktantu a bolo dosiahnuté zlepšenie účinnosti článku o 9% najmä v dôsledku plazmonického zlepšenia prúdu nakrátko. Plazmonické nanočastice boli tiež deponované na rozhranie ITO/aktívna vrstva. Tu je možné okrem plazmonických efektov využiť výrazné zlepšenie faktora vyplnenia z dôvodu lepšieho zberu dier. Takto bolo dosiahnuté 20%-né zlepšenie účinnosti pre 30 nm veľké komerčne dostupné zlaté nanočastice a 10%-né vylepšenie pre zlaté nanočastice vyrobené laserovou abláciou. Opísali sme tiež možnosť nastavenia výstupnej práce ITO substrátu nanosením nanočastíc a následným ožiarением v UV-ozónovom reaktore. Tento efekt sme použili pre zlaté nanotyčinky deponované na rozhranie ITO/PBDTTT-CF:PC<sub>71</sub>BM. Optimalizáciou sme dosiahli zvýšenie napätia naprázdno z 0,72 V na 0,76 V a tiež zvýšenie faktora vyplnenia - v najlepšom prípade znamenajúce zlepšenie účinnosti solárneho článku až o 10% pôvodnej hodnoty. Zaujímavé je, že takmer všetky solárne články so zabudovanými nanočasticami mali zlepšený faktor vyplnenia. Samostatná časť tejto práce pojednáva o štúdiu superhydrofóbných povlakov na báze SiO<sub>2</sub> nanočastíc pre tenkovrstvové fotovoltické články. Po nanosení povlak poskytuje ochrannú a samočistiacu funkciu, ale znížením reflektivity povrchu článku je tiež možné dosiahnuť až 6%-né zlepšenie jeho účinnosti. Počas optimalizácie solárnych článkov sme tiež vyvinuli metódu manipulácie a sledovania zmien perkolovanej štruktúry P3HT:PCBM pomocou ožiarения UV nanosekundovým pulzným laserom a následným skúmaním štruktúry malouhlovým röntgenovým rozptylom (metódy GISAXS a GIWAXS).

Kľúčové slová: organické solárne články, plazmonické nanočastice, laser, superhydrofobicita, výstupná práca

## Abstract

This work deals mainly with an incorporation of different kinds of nanoparticles into an organic photovoltaic structures with an aim to increase their efficiency. The main part of the work is devoted to the use of plasmonic nanoparticles in P3HT:PCBM-based solar cells. We incorporated three types of plasmonic nanoparticles in the organic solar cell active layer: chemically synthesized silver and gold nanoparticles and gold nanoparticles prepared by laser ablation of target in liquid. For chemically synthesized nanoparticles were observed improved values of short-circuit current density. However, observed mechanisms of improvement were different - presumably due to different nanoparticle surfactants. The incorporation of gold nanoparticles worsened fill factor and resulted in lower overall efficiency (with observed plasmonic short-circuit current density improvement) whereas with silver nanoparticles device efficiency was enhanced by 10% but the plasmonic effect on short-circuit current improvement was not proven. With surfactant-free gold nanoparticles, the device efficiency was improved by 9% with main improving effect being enhanced short-circuit current density by localized surface plasmon resonance. The plasmonic nanoparticles were also deposited onto the ITO/active layer interface. Besides the plasmonic effects, we observed significant improvement of fill factor due to better hole collection on the plasmon-enhanced ITO electrode resulting in 20% improvement for 30 nm commercial gold nanoparticles and 10% enhancement for laser-ablated gold nanoparticles. We described work function tuning by depositing nanoparticles on the interface and UV-ozone irradiation. This mechanism was used for gold nanorods deposited on the ITO/PBDTTT-CF:PC<sub>71</sub>BM interface. The nanorods incorporation resulted in increased open-circuit voltage from 0.72 V to 0.76 V and additional fill factor improvement. For the best case, the nanorods improved solar cell efficiency by up to 10% of reference cell. Interestingly, the fill factor improvement was observed for almost all nanoparticle-enhanced devices. An independent part of the work was study of superhydrophobic coating for thin-film solar cells based on SiO<sub>2</sub> nanoparticles. This coating (upon deposition on the top of solar cell) provided not only protective and self-cleaning function but also decreased reflection of the incident light resulted in 6% relative device efficiency improvement. During the solar cell optimization, we described method of manipulation and tracking of P3HT:PCBM bulk heterojunction changes by UV nanosecond pulse laser irradiation and measurement by grazing-incidence small-angle and wide-angle x-ray scattering (GISAXS and GIWAXS).

Keywords: organic solar cell, plasmonic nanoparticles, laser, superhydrophobicity, work function

# Contents

Introduction.....	5
Results .....	7
Simulations.....	7
OSC stability with and without PEDOT:PSS hole transport layer .....	8
UV pulse laser manipulation of P3HT:PCBM bulk heterojunction and tracking by GISAXS and GIWAXS.....	8
Work function tuning by UV/ozone irradiation .....	12
Plasmonic nanoparticles incorporated in the OSC structure .....	13
Superhydrophobic coating for thin film solar cells .....	17
Conclusions.....	19
References.....	22
List of publications.....	23

# Introduction

Over years, the still raising electrical energy demand of the mankind forced scientists to searching for fossil fuel alternatives. Photovoltaic (solar) cells are one of such alternative. As the Sun is a big source of the energy continually irradiating the Earth by ca.  $340 \text{ W}\cdot\text{m}^{-2}$  [1, 2], the solar cells should play a more significant role in future years. The photovoltaic cells is a group containing various kinds of devices with different working principles and achieved efficiencies (**Figure 1**) including inorganic materials such amorphous silicon [3], GaAs [4] or CdTe [5]. The best power conversion efficiency achieved for the most common conventional crystalline silicon solar cells is about 24.7% [6]. The overall record holds a concentrator triple-junction solar cell with an efficiency of 44.4% made by the Sharp Corporation [7].

An environmentally friendly, eventually low-cost alternative to the inorganic solar cells is based on organic semiconductors and is known as organic solar cells. Unfortunately, the state-of-the-art devices are achieving relatively low power conversion efficiencies with the world record of 11.5% for polymer tandem solar cells [8].

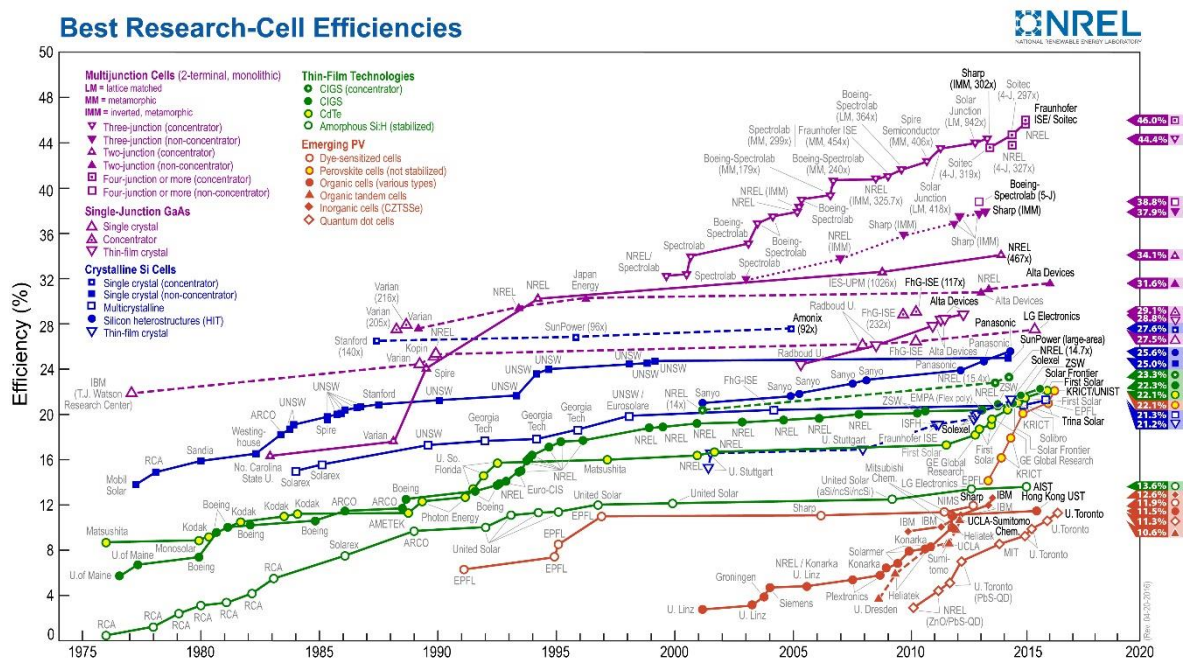


**FIGURE 1** OVERVIEW OF THE BEST RESEARCH-CELL EFFICIENCIES OF VARIOUS TYPES OF SOLAR CELLS [9].

For a reason of yet non-sufficient achieved efficiencies, there is a big effort to increase this value. It is believed that the efficiencies should routinely exceed 10% without complicated production steps to achieve a commercial success. Besides of new chemical compounds synthesis with more convenient electrical properties and optimizing production steps, there is also a possibility to improve the power

conversion efficiency (PCE) by taking advantage of plasmonic properties of small metallic nanoparticles (plasmonic nanoparticles) or various plasmonic nano-structures [10].

For increasing the organic solar cell (OSCs) efficiency, one needs to understand physical and chemical processes ongoing in the device and optimize OSCs parameters to achieve best possible power conversion efficiency for standard architecture before incorporation of nanoparticles. We optimized the device experimentally and also by computer simulations. Subsequently, the optimized solar cell structures were improved by different types of nanoparticles with different functions.

The experimental results consist of OSCs optimization and plasmon-enhanced OSCs results. The plasmonic nanoparticles were incorporated into the solar cell active layer and also at the interface between the active layer and ITO electrode. An importance of nanoparticle surfactant is discussed. The UV nanosecond pulse laser irradiation is not suitable for easy replacement of thermal annealing. However, we described way how to manipulate the P3HT and PCBM separately (in the blend) by UV pulse laser irradiation and tracking the changes by simultaneous GISAXS and GIWAXS measurement.

During the work, we also revealed new possibilities of nanoparticle use in photovoltaic research. By combining deposited metal nanoparticles on the interface active layer/ITO with UV-ozone irradiation, it is possible to tune substrate work function within a broad interval. An applying of superhydrophobic coating (prepared by silicon dioxide nanoparticles) on the top of device did not have only protective and self-cleaning function but also improved solar cell efficiency.

## Results

Despite the use of nanoparticles in organic solar cells (OSCs) being the main aim of the dissertation thesis, one should incorporate nanoparticles only into the optimized structures. In the first part of this chapter, we present results achieved during the OSCs optimization. The nanoparticles were then used in different parts and manner in the optimized OSCs. We employed plasmonic effects of metallic nanoparticles inside the active layer and at the interface ITO/active layer. The nanoparticles deposited at the ITO and subsequently irradiated with UV/ozone allowed to tune the substrate work function. At the end of this chapter, a multifunctional coating based on silica nanoparticles is described.

## Simulations

The computer simulations of optical properties of organic solar cells were performed to help optimize the OSCs structure. To perform the meaningful simulations, it is necessary to use real optical properties of the compounds used in the experiment. The index of refraction and extinction coefficient of glass, ITO, PEDOT:PSS and P3HT:PCBM was obtained from spectroscopic ellipsometry measurements (**Figure 2**).

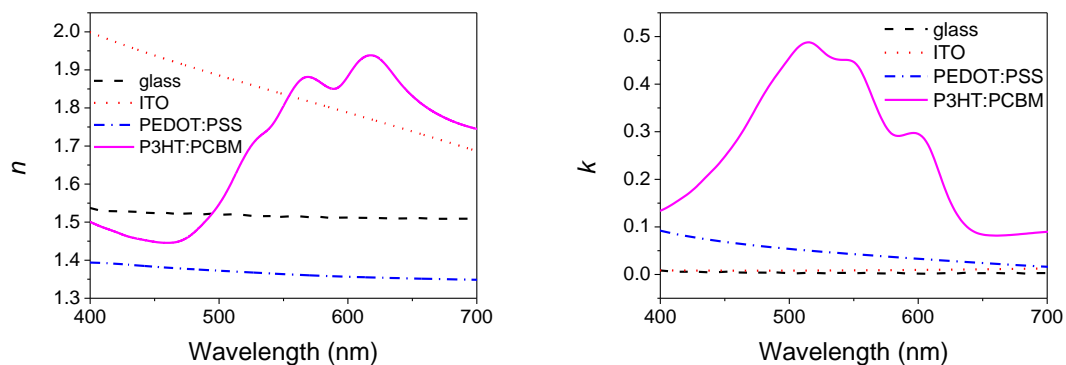


**FIGURE 2** INDEX OF REFRACTION  $n$  AND EXTINCTION COEFFICIENT  $k$  OF MATERIALS USED IN OUR ORGANIC SOLAR CELLS.

The measured optical properties were then used in reflectivity simulations. The simulations were made for P3HT:PCBM and PEDOT:PSS thicknesses as parameters (in the wavelength interval from 400 nm to 700 nm). The simulated reflectivity dependence for device without PEDOT:PSS layer was then correlated with experimental results. The comparison of the simulated reflectivity with the experimental device power conversion efficiency (PCE) dependence can be seen in **Figure 3**. We identified the reflectivity of the OSCs stack as the key parameter in the thickness optimization process. The PCE had the similar shape of the dependence curve as the reflectivity. A slight shift could be ascribed to other parameters such as bulk heterojunction (BHJ) morphology which cannot be included



in the optical simulations. The optimal active layer thickness for P3HT:PCBM-based OSCs was empirically determined to be 110 nm.

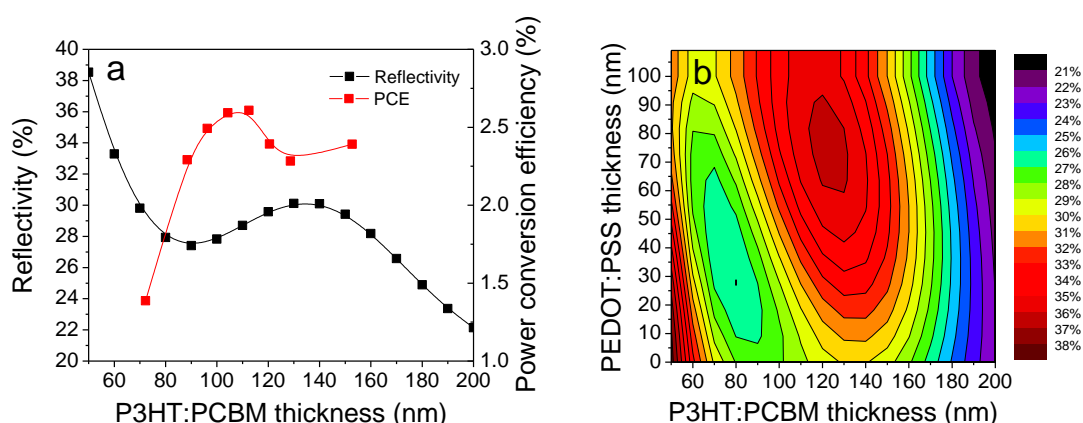


**FIGURE 3** A) COMPARISON OF SIMULATED REFLECTIVITY WITH *PCE* FOR THE SOLAR CELL WITH STRUCTURE GLASS/400 NM ITO/P3HT:PCBM/CA/AG. MODIFIED FROM [11]. B) COMPUTED REFLECTIVITY OF OSC WITH 400 NM ITO THICKNESS AND P3HT:PCBM AND PEDOT:PSS THICKNESSES AS PARAMETERS.

## OSC stability with and without PEDOT:PSS hole transport layer

The organic solar cells based on PBDTTT-EFT/PCB<sub>71</sub>M with and without hole transport layer PEDOT:PSS were prepared by standard production procedure and encapsulated by encapsulation epoxy. The both devices were measured fresh prepared and after 2 hours, 6, 24, 43 and 77 days. The basic parameters evolution as a function of time is depicted in **Figure 4**. The similar initial efficiency value can be achieved either by use of PEDOT:PSS or by irradiation of the ITO in UV/ozone reactor which tuned the ITO work function to the same value as the PEDOT:PSS have. Despite the similar initial PCE, we observed bigger PCE decrease and worse stability for the sample without PEDOT:PSS during the time. This was attributed to oxygen atoms introduced by UV/ozone irradiation at the ITO which can diffuse to the active layer causing worsening of the device parameters.

## UV pulse laser manipulation of P3HT:PCBM bulk heterojunction and tracking by GISAXS and GIWAXS

We studied possibilities of replacement of solvent and thermal annealing steps required for P3HT:PCBM-based OSCs for achieving high efficiency. The UV pulse laser (355 nm) irradiation was used to manipulate the BHJ morphology. The P3HT:PCBM layers spin-coated onto the silicon substrates were irradiated by the laser with different laser fluencies from 0.5 to 2.0 mJ.cm<sup>-2</sup>. The changes induced by the irradiation were inspected by the simultaneous grazing-incidence small-angle and wide-angle x-ray scattering (GISAXS and GIWAXS) at the synchrotron in NSRRC, Taiwan. We were able to

differentiate between the P3HT crystallization and PCBM aggregation as well as manipulate the both phases separately.

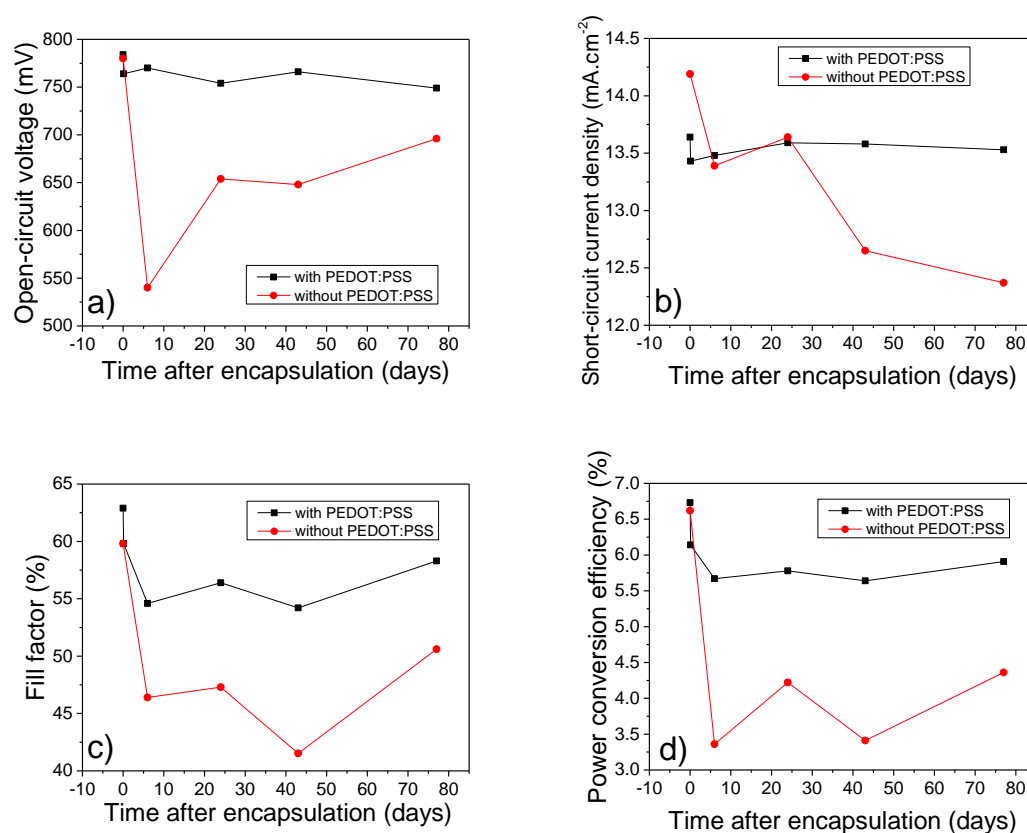


**FIGURE 4** AN OVERVIEW OF OSCS PARAMETERS AS A FUNCTION OF TIME AFTER ENCAPSULATION. A COMPARISON OF OSCS WITH AND WITHOUT THE PEDOT:PSS. THE DEVICE WITH PEDOT:PSS HAD LOWER EFFICIENCY DROP COMPARED WITH OSC WITHOUT PEDOT:PSS.

### P3HT crystallization and PCBM aggregation tracking

For tracking of the changes in P3HT phase after the laser treatment, we evaluated 100 P3HT diffraction peak. We fitted the peak with a Gaussian and evaluated changes in the peak parameters relative to the corresponding reference sample. The relative peak area change after laser irradiation is shown in **Figure 5a**. We observed enhanced peak area approximately in interval from 0.6 to 1.0 mJ.cm<sup>-2</sup> with maximum enhancement being at 0.8 mJ.cm<sup>-2</sup>. The area is proportional to scattering volume thus its enhancement indicates bigger scattering volume created either by crystallites nucleation of new or growth of the existing domains. At higher laser fluencies (above 1.2 mJ.cm<sup>-2</sup>) it came to decrease of peak area indicating degradation of the sample. An additional information about crystallinity, namely crystal size provides peak full width at half maximum (FWHM). A narrowing of the P3HT 100 peak was observed in the same laser fluence region as was peak area enhancement (**Figure 5b**). The narrowing of the peak corresponded to P3HT crystal growth from initial 13.7 nm to 14.6 nm for 0.8 mJ.cm<sup>-2</sup>

irradiation. This value corresponds well with optimal P3HT domain size for best solar cell efficiency [12].

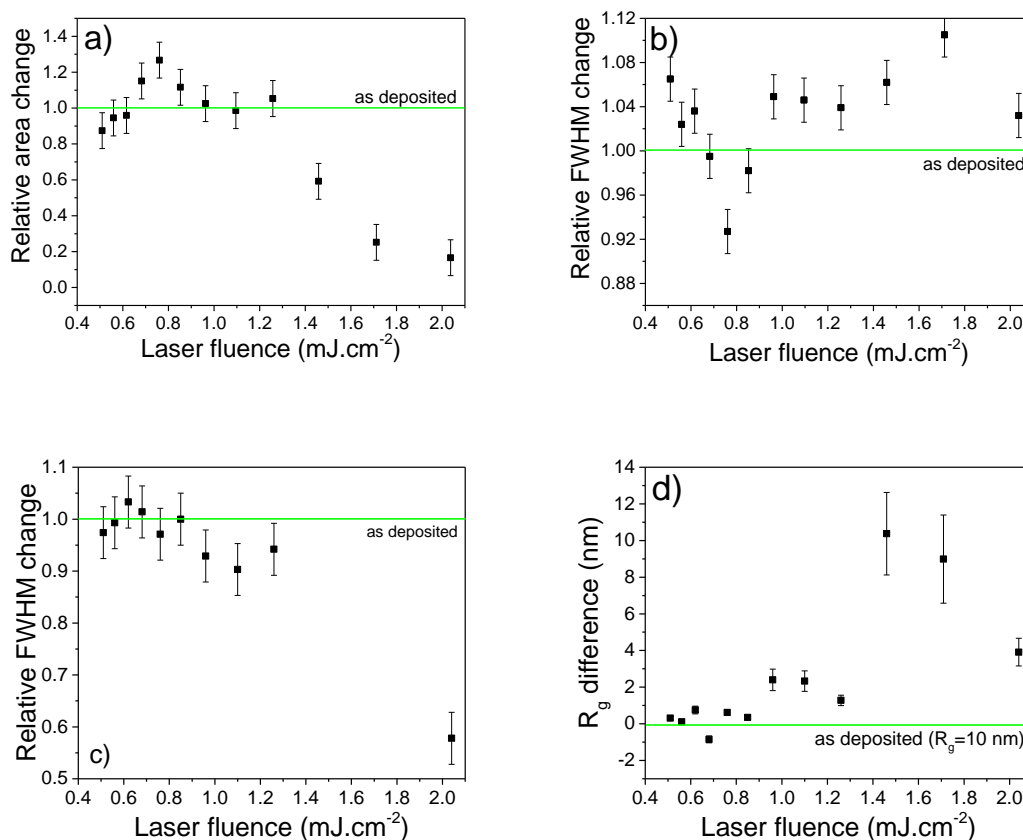


**FIGURE 5** EVALUATED PARAMETERS FROM GIWAXS AND GISAXS MEASUREMENTS. THE RELATIVE A) AREA AND B) FWHM CHANGE OF THE P3HT 100 PEAK AS A FUNCTION OF THE LASER FLUENCE. THE P3HT CRYSTALLIZATION ENHANCEMENT, PEAKED AT 0.8 MJ.CM<sup>-2</sup>, IS VISIBLE BY PEAK AREA INCREASE ACCOMPANIED BY ITS NARROWING. THE NARROWING OF THE GISAXS PEAK (C) AND ENHANCEMENT OF THE RADIUS OF GYRATION (D) IS OBSERVED FOR PCBM AGGREGATION WITH MAXIMUM AT AT 1.1 MJ.CM<sup>-2</sup>.

The similar analysis was performed also for GISAXS peak characterizing BHJ percolated structure. We observed sudden changes of the peak area and position when it came to sample damage at high laser fluences where it was not possible to fit the peak – peak almost disappeared. The significant changes were visible only on GISAXS peak FWHM **Figure 5c**. No changes were visible until 0.9 mJ.cm<sup>-2</sup> indicating no agglomeration of PCBM molecules. Between 0.9 mJ.cm<sup>-2</sup> and ca. 1.3 mJ.cm<sup>-2</sup> was observed narrowing of the peak with maximum narrowing to 90% of reference width at 1.1 mJ.cm<sup>-2</sup>. For proving the PCBM agglomeration, we performed the Guinier analysis. The scattered intensity in the low-*q* region is dominated mainly by large PCBM aggregates [13]. The radius of gyration *R<sub>g</sub>* of PCBM aggregates can be determined from the Guinier plot, keeping the conditions for evaluated region:  $qR_g < 1.3$  and the region must lie outside the GISAXS peak. The change of the *R<sub>g</sub>* as a function of the laser fluence is depicted in **Figure 5d**. No changes were observed up to 0.9 mJ.cm<sup>-2</sup> where the *R<sub>g</sub>*

started to increase. The maximum increase of 2.5 nm from the initial value of 10 nm was observed at around  $1.1 \text{ mJ.cm}^{-2}$ . At the laser fluencies higher than  $1.5 \text{ mJ.cm}^{-2}$  it came to dramatic enlargement of PCBM radius of gyration by up to 11 nm.

### P3HT crystallization and PCBM aggregation in terms of energy

Wu et al. [14] describes the phase separation mechanism in terms of nucleation and subsequent growth requiring some activation energy. However, as seen from our results above, both the P3HT crystallization and PCBM agglomeration processes had bell-shape curve character. This is generally true for macromolecular crystals [15]. Therefore speaking about activation energies is not quite correct. One should rather speak about energy interval for the process to occur. We evaluated the energy required for maximum P3HT crystallization and PCBM aggregation. For maximum of PCBM aggregation at laser fluence  $1.0 \text{ mJ.cm}^{-2}$  the delivered energy is  $80 \text{ kJ.mol}^{-1}$ . This is  $0.83 \text{ eV}$  per 1 PCBM molecule what corresponds well with the values for molecular diffusion in polymers ( $0.52 \text{ eV} - 0.83 \text{ eV}$ ) [16, 17] and is also close to measured value of  $0.68 \text{ eV}$  per molecule for low-content (<1%) disordered PCBM in P3HT:PCBM systems [18]. The experimental value for PCBM agglomerates diffusion is almost two times larger [19], therefore the laser-induced process was PCBM agglomeration due to individual PCBM molecules diffusion. For P3HT maximum of crystallization, the laser fluence  $0.78 \text{ mJ.cm}^{-2}$  corresponds to  $2568 \text{ kJ.mol}^{-1}$  ( $26.62 \text{ eV}$  per polymer chain). This value is quite high due to high molecular weight of the P3HT polymer (calculated average value of  $64.5 \text{ kg.mol}^{-1}$ ). For clean polymer in powder form, the value of  $319 \text{ kJ.mol}^{-1}$  was reported [20]. The enthalpy of fusion of P3HT ideal crystal was, however, measured to be ca.  $98 \text{ J.g}^{-1}$  [21] being  $6386 \text{ kJ.mol}^{-1}$  for P3HT molecular weight used in our experiment. Our value lays in the broad interval between these two values. We have no knowledge of measuring the required energy per polymer chain for P3HT crystallization in P3HT:PCBM BHJ systems.

### Raman spectroscopy

We correlated the previous results with the non-resonant Raman spectroscopy. In **Figure 6** is shown a Raman spectrum of as-deposited P3HT:PCBM layer. There are different peaks corresponding to different Raman modes. The peak at  $1170 \text{ cm}^{-1}$  defined by the inter-molecular bond forming the polymer chain should be the most sensitive probe to study changes of the P3HT.

The evaluated position of the peak (**Figure 7a**) revealed its shifting to higher wavenumbers (energies) in the same laser fluence interval where the PCBM aggregation occurred. This corresponds to shortening of the  $\text{C}_\alpha\text{-C}_\alpha$  bond. We suggested that this shift is due to diffusion of PCBM molecules outside of the P3HT matrix (and polymer chains relaxation) resulting in pure P3HT domains around the PCBM agglomerates. This was also supported by a peak broadening (**Figure 7b**) probably resulting from

these newly created pure P3HT domains around the PCBM agglomerates introducing new states and disorder to the system.

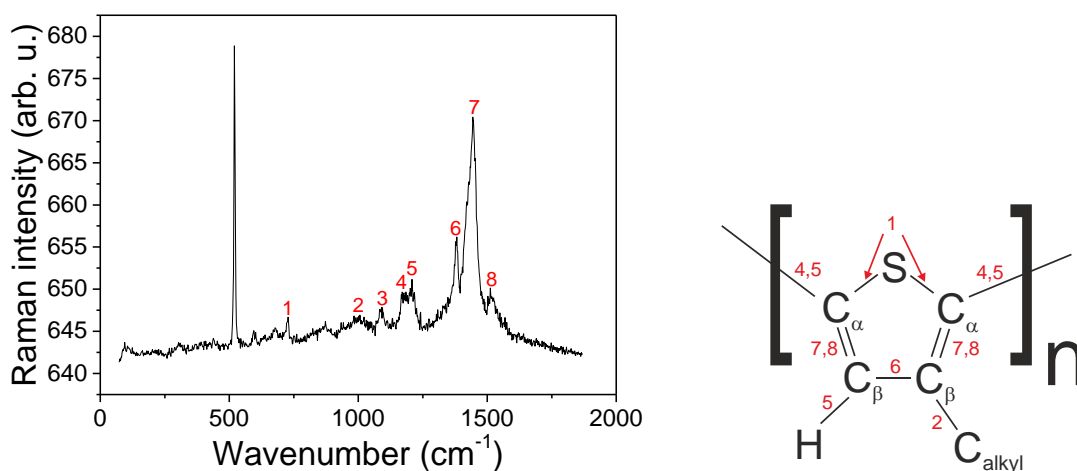


**FIGURE 6** OFF-RESONANT RAMAN SPECTRUM (AT 785 NM EXCITATION WAVELENGTH) OF AS-DEPOSITED SAMPLE OF P3HT:PCBM BHJ SYSTEM. THE BONDS FORMING THE PEAKS ARE MARKED IN THE P3HT SCHEMATIC PICTURE.

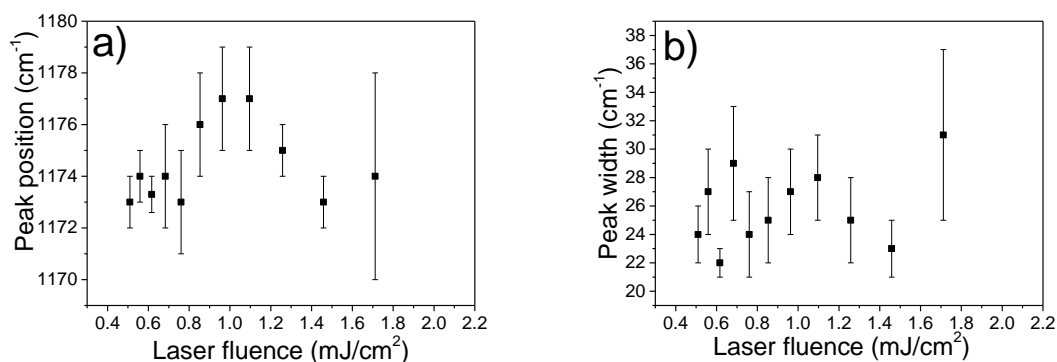


**FIGURE 7** THE EVALUATION OF PEAK CORRESPONDING TO  $C_A-C_A$  SYMMETRIC STRETCHING MODE FROM RAMAN SPECTRA. A) THE PEAK SHIFT WAS OBSERVED IN THE SAME REGION AS THE PCBM AGGLOMERATION. THE CLAIM THAT THE SHIFT IS INDUCED BY REMOVING THE PCBM MOLECULES FROM THE P3HT MATRIX RESULTING IN PURE P3HT DOMAINS AROUND THE AGGLOMERATES IS SUPPORTED BY THE BROADENING OF THE PEAK (B).

## Work function tuning by UV/ozone irradiation

The work function of the ITO electrode can be tuned by UV/ozone irradiation ca. from -5.0 eV to -5.5 eV. By adding the gold nanoparticles before the irradiation, the tuning interval can be broadened almost twice from -4.7 eV to -5.8 eV. The work function dependence as a function of UV/ozone irradiation time for the bare ITO and ITO with deposited gold spherical nanoparticles and nanorods can be seen in **Figure 8**.

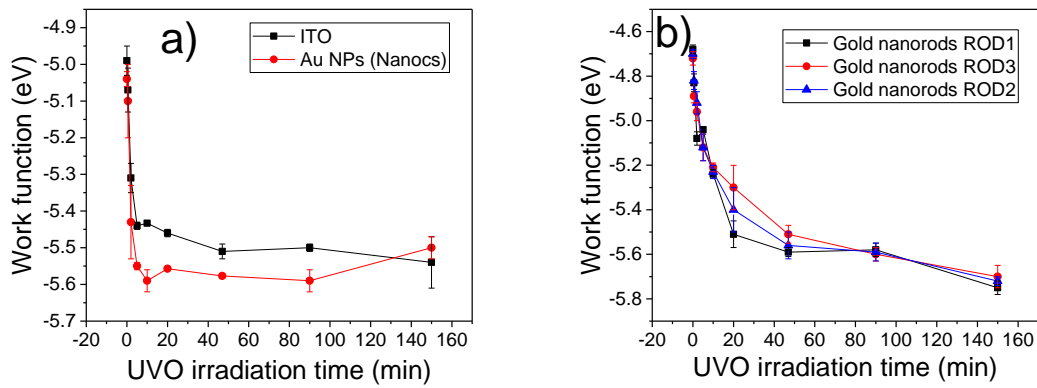


**FIGURE 8** WORK FUNCTION DEPENDENCE ON THE UV/OZONE TREATMENT TIME OF (A) BARE ITO (SQUARES) AND ITO WITH GOLD NANOCs NPs (CIRCLES) AND (B) ITO WITH ROD1 (SQUARES), ROD2 (CIRCLES), ROD3 (TRIANGLES) NANORODS DEPOSITED UNDER THE OPTIMIZED *PCE* CONDITIONS. THE LINES ARE GUIDES TO THE EYE. ADAPTED FROM [22].

## Plasmonic nanoparticles incorporated in the OSC structure

The plasmonic nanoparticles were incorporated in the active layer and also at the ITO/active layer interface. We incorporated the gold and silver nanoparticles with the aim of employing localized surface plasmon resonance (LSPR) effect. The LSPR causes a big enhancement of electric field intensity in a close vicinity of the nanoparticle (**Figure 9**). This enhancement should result in higher absorption of incoming photons and thus increases electric current provided by the OSCs. The nanoparticles are, however, usually prepared by chemical synthesis and the individual nature of the nanoparticles is ensured by the use of surfactants covering the nanoparticle surface. The surfactant weakens the near-field plasmonic effect and can also interact with the active layer compounds.

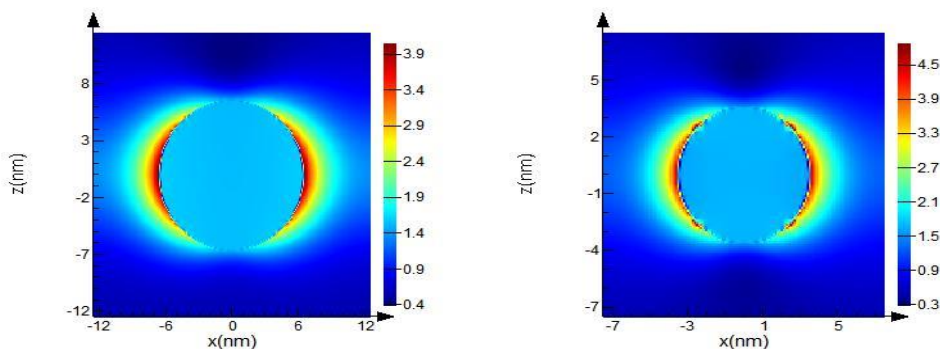


**FIGURE 9** FDTD SIMULATIONS OF ENHANCED ELECTRIC FIELD INTENSITY AROUND NANOPARTICLES DUE TO LSPR OF 13 NM SILVER (LEFT) AND 6 NM GOLD (RIGHT) NANOPARTICLE INCORPORATED IN P3HT:PCBM ACTIVE LAYER.

In the active layer volume, we incorporated two types of chemically synthesized nanoparticles. The 13 nm silver nanoparticles using the oleic acid as a surfactant and 6 nm gold nanoparticles covered by

mixture of mercaptoalcanes. We observed different effects introduced by the nanoparticles. By gold nanoparticles, the short-circuit current density of the device was improved but the overall PCE was worsened due to decrease of device fill factor. The analysis of exciton generation rate and exciton dissociation probability (together with EQE measurement) revealed that more excitons were generated due to LSPR, however the nanoparticles acted like recombination centers. With the silver nanoparticles, we achieved increased short-circuit current density together with the overall efficiency improvement. The improvement, unfortunately, was not caused by the LSPR.

We produced surfactant-free gold nanoparticles by laser ablation of gold target in liquid to avoid the surfactant influence. The laser ablation is up to date only method how to prepare nanoparticle solution without any chemical additives. The nanoparticles prepared by laser ablation agglomerated after dropping on the silicon substrate but preserved individual nature when spin-coated onto the ITO substrate (**Figure 10**).

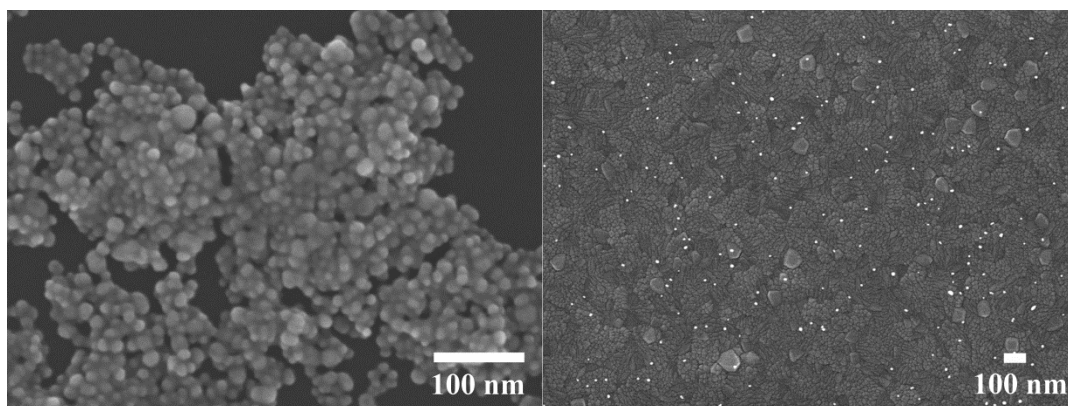


**FIGURE 10** CHEMICALLY CLEAN GOLD NANOPARTICLES (PREPARED BY LASER ABLATION) AGGLOMERATED AFTER DROP CASTING ONTO SILICON SUBSTRATE (LEFT) AND WITH PRESERVED INDIVIDUAL CHARACTER AFTER SPIN-COATING ON THE ITO SUBSTRATE (RIGHT).

By the use of laser-ablated nanoparticles, we achieved increased short-circuit current density together with the PCE enhancement. The short-circuit current density increase was highest at around 550 nm which corresponded well with the plasmonic absorption peak (LSPR maximum). The exciton generation rate and also exciton dissociation probability was improved. The relative PCE enhancement was 9%. The representative electrical measurement results for surfactant-free nanoparticles can be seen in **Figure 11**.

We incorporated nanoparticles also at the ITO/active layer interface. Here, one can combine LSPR effect with the work function tuning described above. Also scattering on the nanoparticles have bigger influence in this case. We used two types of gold spherical nanoparticles in the P3HT:PCBM-based OSC. For gold nanorods incorporation, we chose the active layer consisting of low band-gap polymer PBDTTT-CF and the PC<sub>71</sub>BM. This polymer can absorb in the higher wavelengths region and better

overlaps with the nanorods longitudinal LSPR mode. The best results were achieved by incorporation of the 30 nm gold nanoparticles purchased from Nanocs company (**Figure 12**). Here, the plasmonic enhancement of the short-circuit current density together with the other improved parameters was observed. The changes in open-circuit voltage values were also achieved by the work function tuning. For these nanoparticles, the best overall improvement of the device efficiency was achieved. The PCE was improved by 20% from 2.52% to 3.02%. The all results with the incorporation of nanoparticles are listed in **Table 2**.

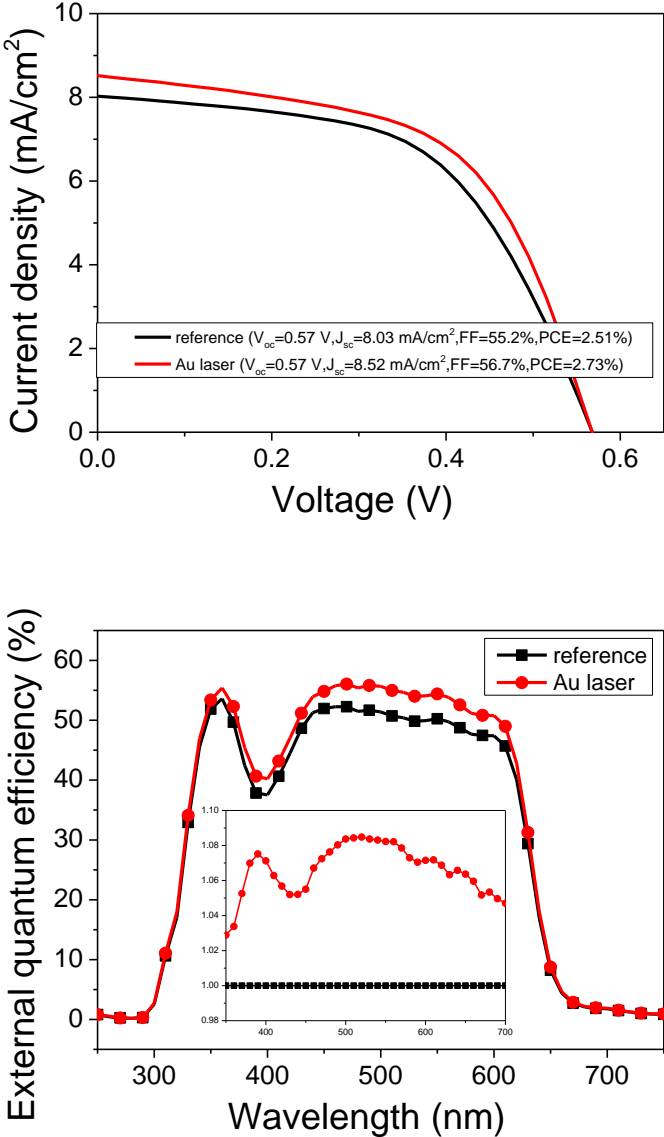


**FIGURE 11** THE SOLAR CELL  $J - V$  CURVES WITH INCORPORATED LASER-ABLATED GOLD NANOPARTICLES (TOP) WITH CORRESPONDING EXTERNAL QUANTUM EFFICIENCY CURVES (BOTTOM, RELATIVE EXTERNAL QUANTUM EFFICIENCY AS AN INSET). A 9% *PCE* RELATIVE IMPROVEMENT WAS ACHIEVED MAINLY DUE TO 6% SHORT-CIRCUIT CURRENT DENSITY INCREASE.



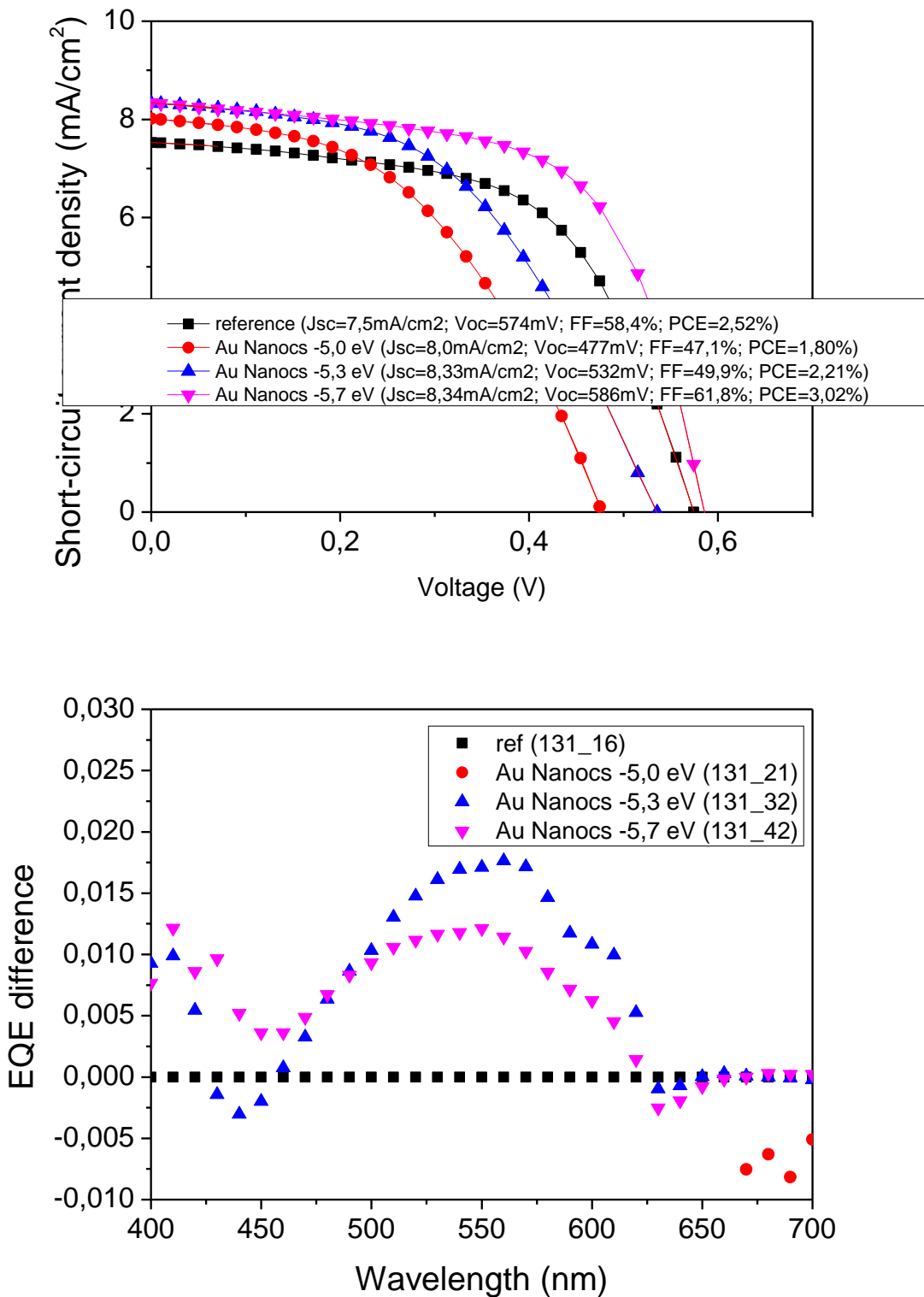


**FIGURE 12J** –  $V$  CURVES OF OSCs WITH INCORPORATED 30 NM GOLD NANOPARTICLES ON THE ITO/ACTIVE LAYER INTERFACE (TOP). THE NANOPARTICLES TOGETHER WITH UVO IRRADIATION WERE USED TO SET THE SUBSTRATE WORK FUNCTION TO -5.0, -5.3 AND -5.7 eV RESULTING IN DIFFERENT  $V_{oc}$  VALUES. THE LSPR WAS OBSERVED RESULTING IN  $J_{sc}$  ENHANCEMENT WITH MAXIMUM  $EQE$  IMPROVEMENT AT 550 NM (BOTTOM).

## Superhydrophobic coating for thin film solar cells

As another use of nanoparticles in the OSCs structure we presented the use of superhydrophobic coating based on the functionalized  $\text{SiO}_2$  nanoparticles. This coating can be generally used in all thin film solar cells. The rough surface of the coating provided not only the protective function by the superhydrophobic effects (**Figure 13**) but also decreased the reflectivity of the OSC surface and thus increased the short-circuit current density. The corresponding J-V curves are depicted in **Figure 14**.

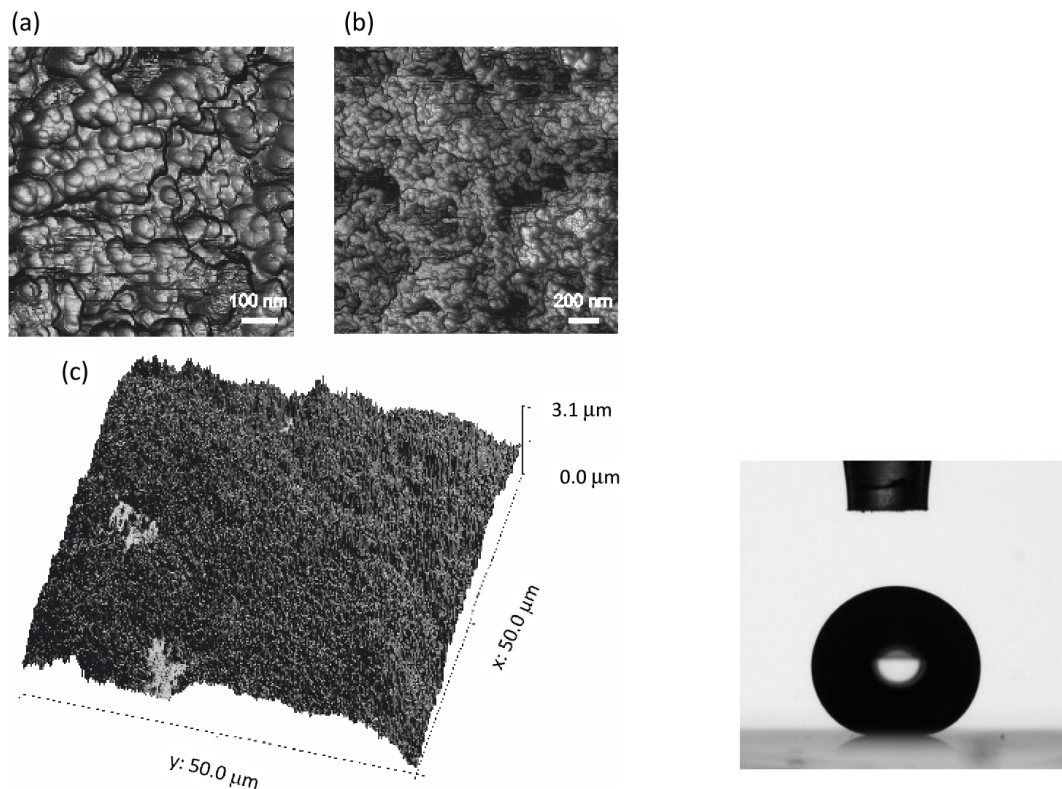


**FIGURE 13** AFM STUDY OF SUPERHYDROPHOBIC  $\text{SiO}_2$ +OTS MONOLAYER MORPHOLOGY (LEFT). THE WATER DROPLET ON THE SUPERHYDROPHOBIC SURFACE (RIGHT).

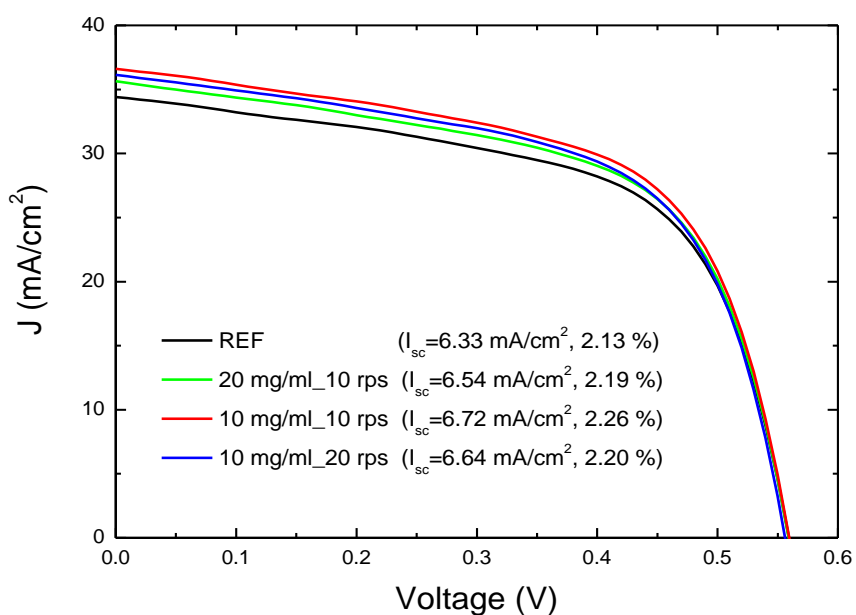


**FIGURE 14** CURRENT DENSITY – VOLTAGE CURVES OF THE OSCS WITHOUT AND WITH THE SUPERHYDROPHOBIC COATING BASED ON  $\text{SiO}_2$  NANOPARTICLES. THE POWER CONVERSION EFFICIENCY IMPROVEMENT WAS OBSERVED DUE TO SHORT-CIRCUIT CURRENT DENSITY ENHANCEMENT BY THE SURFACE REFLECTIVITY DECREASE.

Coating	Nanoparticle concentration (mg/ml)	Rotation speed (rps)	$J_{sc}$ (mA/cm <sup>2</sup> )	$U_{oc}$ (mV)	FF (%)	PCE (%)
None	---	---	6.33	559	60.2	2.13
#1	20	10	6.54	559	60.1	2.19
#2	10	10	6.72	559	60.1	2.26
#3	10	20	6.64	556	59.7	2.20

**TABLE 1** THE PARAMETERS OF THE OSC WITH SPIN-COATED SUPERHYDROPHOBIC LAYERS AS DETERMINED FROM  $J - V$  CURVES.

## Conclusions

We studied the effect of application of metallic nanoparticles in the organic photovoltaic structures. The main part of this work was devoted to use of plasmonic nanoparticles in order to increase the device power conversion efficiency. The optimization and stability study of the structure was performed as well. In this thesis we described effects of thermal and solvent annealing on the bulk heterojunction structures, empirical and simulation-based OSCs optimization, as well as UV nanosecond pulse laser manipulation of bulk heterojunction and use of nanoparticles in different ways in the OSCs structure. We used plasmonic effects in the active layer to increase incoming light absorption and increase short-circuit current density. Deposited at the ITO/active layer interface, spherical nanoparticles and nanorods were (combined with UV-ozone irradiation) to tune the substrate work function. We developed the superhydrophobic coating based on SiO<sub>2</sub> nanoparticles which can be deposited on the top of the OSCs and provides not only protective and self-cleaning function but also decreases reflection of incoming light and thus enhances absorption, short-circuit current density and efficiency of the solar cell.

The optical constants of the various elements of organic solar cell were determined by ellipsometry. These values were used in numerical simulations. We performed simulation of OSC stack reflectivity as a function of active layer and hole transport layer thicknesses. The reflectivity was identified as a key factor in efficiency optimization.

As alternative approach to conventional solvent/thermal annealing, the irradiation of P3HT:PCBM blend by UV nanosecond pulse laser was studied at the wavelength of 355 nm. The samples were then inspected by simultaneous grazing-incidence small angle and wide angle x-ray scattering (GISAXS and GIWAXS). These studies were completed by off-resonant Raman scattering spectroscopy.

By nanosecond laser irradiation with different laser fluencies, we were able to track and differentiate between the P3HT crystallization and PCBM aggregation. The differentiation of these two processes is possible only by ultra-short nature of the pulse laser irradiation providing specific temperature in ultra-short time. By conventional hot-plate annealing, the processes occurring at higher temperatures are influenced by lower-temperature states through which the system is passing.

We performed also stability study on encapsulated organic solar cells based on high-performance, low-band gap polymer PBDTTT-EFT. The device with and without a hole transport layer PEDOT:PSS were compared for 77 days. The OSC with PEDOT:PSS layer was more stable over time and maintained ca. 86% of its initial efficiency value (6.7%).

Sample	Voc [V]	Jsc [mA.cm <sup>-2</sup> ]	FF [%]	PCE [%]	PCE relative improvement [%]	Gmax [10 <sup>27</sup> m <sup>-3</sup> s <sup>-1</sup> ]	P(E,T) [%]
NPs in the active layer							
Reference	0.58	8.06	64.5	3.03	0	3.481	90.6
Au Plasmachem	0.55	<b>8.63</b>	51.6	2.50	-17.5	<b>4.795</b>	70.5
Reference	0.58	8.63	57.6	2.90	0	4.554	87.7
AgCl	0.58	<b>9.02</b>	<b>59.9</b>	<b>3.20</b>	<b>10.3</b>	4.551	<b>91.5</b>
Reference	0.57	8.03	55.2	2.51	0	4.552	94
Au laser	0.57	<b>8.52</b>	<b>56.7</b>	<b>2.73</b>	<b>8.8</b>	<b>4.830</b>	<b>95.6</b>
NPs at ITO/active layer interface							
Reference	0.57	7.50	58.4	2.52	0	4.54	94.1
Au Nanocs	<b>0.59</b>	<b>8.64</b>	<b>61.8</b>	<b>3.02</b>	<b>19.8</b>	<b>4.99</b>	<b>94.8</b>
Reference	0.56	8.11	56.6	2.58	0	5.11	90.0
Au laser	<b>0.57</b>	7.84	<b>63.6</b>	<b>2.84</b>	<b>10.1</b>	4.71	<b>94.4</b>
Reference	0.72	12.24	53.9	4.80	0	7.66	90.5
ROD1	<b>0.76</b>	12.20	<b>55.7</b>	<b>5.13</b>	<b>6.9</b>	7.54	<b>91.6</b>
ROD2	<b>0.76</b>	<b>12.34</b>	<b>56.4</b>	<b>5.27</b>	<b>9.8</b>	7.66	<b>91.4</b>
ROD3	<b>0.76</b>	<b>12.27</b>	53.9	<b>5.00</b>	<b>4.2</b>	<b>7.71</b>	90.1
Superhydrophobic coating							
Reference	0.56	6.33	60.2	2.13	0		
Coating	0.56	<b>6.72</b>	60.1	<b>2.26</b>	<b>6.1</b>		

**TABLE 2** THE OVERVIEW OF ORGANIC SOLAR CELLS PARAMETERS WITH INCORPORATED NANOPARTICLES. IMPROVED PARAMETERS RELATIVE TO REFERENCE CELL ARE LISTED IN BOLD.

By irradiation of ITO substrate in an UV/ozone reactor we broadened work function tuning interval. With adding nanoparticles on top of ITO, we broadened the tuning interval almost twice – it is possible to tune work function from -4.7 eV to -5.7 eV.

The enhancements of OSCs parameters by using nanoparticles are listed in **Table 2**. We proved a possibility of employing plasmonic effect on small metal nanoparticles upon incorporation into the

active layer of the solar cell. Here, the nanoparticle surfactant played important role and determined whether the exciton creation was improved or excitons were dissociated. For the silver nanoparticle was achieved best results with device efficiency improvement by up to 10% from 2.9% to 3.2%. However, the improvement was achieved by increased exciton dissociation probability presumable due to suitable surfactant. As an ideal surfactant turned to be no surfactant and the surfactant-free gold nanoparticles prepared by laser ablation of metal target in liquid increased both the generation and dissociation probability of excitons. This resulted in 9% relative *PCE* enhancement.

The plasmonic nanoparticles at the ITO/active layer interface could be used for localized surface plasmon resonance – increased short-circuit current density or for substrate work function tuning by UV-ozone irradiation – increased open-circuit voltage. Both advantages were combined only in one case – 30 nm gold nanoparticles (Nanocs) where enhancement of all OSC parameters resulted in highest achieved improvement by almost 20%. The other used nanoparticles acted more like dissociation centers for excitons increasing fill factor and overall device efficiency. The nanorods acted similarly to spherical nanoparticles.

The superhydrophobic coating based on silica nanoparticles was developed and used on organic solar cell. The coating provided not only protective and self-cleaning function but also decreased reflection of incoming light – increased light absorption in the active layer. After optimization, we were able to achieve up to 6% power conversion efficiency improvement.

## References

1. Kopp, G. and J.L. Lean, *A new, lower value of total solar irradiance: Evidence and climate significance*. Geophysical Research Letters, 2011. **38**.
2. NASA\_Earth\_Observatory. *Incoming sunlight*. 2014 [cited 2014 January]; Available from: <http://earthobservatory.nasa.gov/Features/EnergyBalance/page2.php>.
3. Green, M.A., *Recent developments in photovoltaics*. Solar Energy, 2004. **76**(1-3): p. 3-8.
4. Bauhuis, G.J., et al., *26.1% thin-film GaAs solar cell using epitaxial lift-off*. Solar Energy Materials and Solar Cells, 2009. **93**(9): p. 1488-1491.
5. Romeo, A., et al., *Development of thin-film Cu(In,Ga)Se-2 and CdTe solar cells*. Progress in Photovoltaics, 2004. **12**(2-3): p. 93-111.
6. Zhao, J., A. Wang, and M.A. Green, *High-efficiency PERL and PERT silicon solar cells on FZ and MCZ substrates*. Solar Energy Materials and Solar Cells, 2001. **65**(1-4): p. 429-435.
7. Sharp. 2013 2016]; Available from: <http://sharp-world.com/corporate/news/130614.html>.
8. Chen, C.C., et al., *An Efficient Triple-Junction Polymer Solar Cell Having a Power Conversion Efficiency Exceeding 11%*. Advanced Materials, 2014. **26**(32): p. 5670-+.
9. NREL. *Best Research-Cell Efficiencies*. Available from: [http://www.nrel.gov/ncpv/images/efficiency\\_chart.jpg](http://www.nrel.gov/ncpv/images/efficiency_chart.jpg).
10. Gan, Q.Q., F.J. Bartoli, and Z.H. Kafafi, *Plasmonic-Enhanced Organic Photovoltaics: Breaking the 10% Efficiency Barrier*. Advanced Materials, 2013. **25**(17): p. 2385-2396.
11. Kaiser, M., *Study of Organic Photovoltaic Systems*. 2013: Bratislava.
12. Chiu, M.Y., et al., *Morphologies of Self-Organizing Regioregular Conjugated Polymer/Fullerene Aggregates in Thin Film Solar Cells*. Macromolecules, 2010. **43**(1): p. 428-432.
13. Chiu, M.Y., et al., *Simultaneous use of small- and wide-angle X-ray techniques to analyze nanometerscale phase separation in polymer heterojunction solar cells*. Advanced Materials, 2008. **20**(13): p. 2573-+.
14. Wu, W.R., et al., *Competition between Fullerene Aggregation and Poly(3-hexylthiophene) Crystallization upon Annealing of Bulk Heterojunction Solar Cells*. ACS Nano, 2011. **5**(8): p. 6233-6243.
15. Wunderlich, B., *Macromolecular physics*. 1973, New York: Academic Press.
16. Neogi, P., *Diffusion in polymers*. Plastics engineering. 1996, New York: Marcel Dekker. ix, 309 p.
17. Berens, A.R. and H.B. Hopfenberg, *Diffusion of organic vapors at low concentrations in glassy PVC, polystyrene, and PMMA*. Journal of Membrane Science, 1982. **10**(2): p. 283-303.
18. Treat, N.D., et al., *Temperature Dependence of the Diffusion Coefficient of PCBM in Poly(3-hexylthiophene)*. Macromolecules, 2013. **46**(3): p. 1002-1007.
19. Berriman, G.A., et al., *Molecular versus crystallite PCBM diffusion in P3HT:PCBM blends*. Aip Advances, 2015. **5**(9).
20. Yang, Z.P. and H.B. Lu, *Nonisothermal Crystallization Behaviors of Poly(3-hexylthiophene)/Reduced Graphene Oxide Nanocomposites*. Journal of Applied Polymer Science, 2013. **128**(1): p. 802-810.
21. Malik, S. and A.K. Nandi, *Crystallization mechanism of regioregular poly(3-alkyl thiophene)s*. Journal of Polymer Science Part B-Polymer Physics, 2002. **40**(18): p. 2073-2085.
22. Vojtko, A., et al., *Towards organic solar cells without the hole transporting layer on the plasmon-enhanced ITO electrode*. Physica Status Solidi a-Applications and Materials Science, 2015. **212**(4): p. 867-876.

## List of publications

Citation listed in CC – blue

Citation in doctoral thesis - red

Citation in conference contribution – green

### Publications in CC journals:

2015:

- ŠIFFALOVIČ, Peter - BADANOVÁ, Dominika - VOJTKO, Andrej - JERGEL, Matej - HODAS, Martin - PELLETTA, Marco - SABOL, D. - MACHA, M. - MAJKOVÁ, Eva. **Evaluation of low-cadmium ZnCdS<sub>2</sub> alloyed quantum dots for remote phosphor solid-state lighting technology.** In *Applied Optics*, 2015, vol. 54, no. 23, p. 7094-7098.
  - JAMSHIDI ZAVARAKI, Asghar. **Engineering Multicomponent Nanostructures for MOSFET, Photonic Detector and Hybrid Solar Cell Applications.** In Doctoral Thesis, KTH Royal Institute of Technology, Stockholm, 2015.
- VOJTKO, Andrej - JERGEL, Matej - NÁDAŽDY, Vojtech - ŠIFFALOVIČ, Peter - KAISER, Michal - HALAHOVETS, Yuriy - BENKOVIČOVÁ, Monika - IVANČO, Ján - MAJKOVÁ, Eva - EROLA, Markus O.A. - SUVANTO, S. - PAKKANEN, Tuula T. **Towards organic solar cells without the hole transporting layer on the plasmon-enhanced ITO electrode.** In *Physica Status Solidi A*, 2015, vol. 212, no. 4, p. 867-876.
  - MULLEROVA, J. – KAISER, M. – NADAZDY, V. – SIFFALOVIC, P. – MAJKOVA, E. **Optical absorption study of P3HT:PCBM blend photo-oxidation for bulk heterojunction solar cells.** In *Solar Energy*, 2016, vol. 134, p. 294-301.
  - BOULANGER, Nicolas. **Carbon nanotubes and graphene polymer composites for opto-electronic applications.** In Doctoral Thesis, Umea universitet, Umea, 2016.
  - MULLEROVA, J. – NADAZDY, V. – SCHOLTZ, L. – LADANYI, L. **On pristine and blend optical absorption in new-generation low band-gap organic semiconductors for heterojunction solar cells.** In APCOM 2015: Proceedings of the 21<sup>st</sup> International Conference on Applied Physics of Condensed Matter. Eds. J. Vajda, I. Jamnicky; rev. J. Sitek, P. Ballo et al. – Bratislava : STU, 2015, p. 338-341.
  - BENKOVIČOVÁ, M. - KOTLÁR, M. - VOJTKO, A. - JERGEL, M. - ŠIFFALOVIČ, P. - VÉGSO, K. - LUBY, Š. - MAJKOVÁ, E. **Synthesis of gold nanorods with different aspect ratio for organic photovoltaics.** In APCOM 2015 : Proceedings of the 21st International Conference on Applied Physics of Condensed Matter. Eds. J. Vajda, I. Jamnický ; rev. J. Sitek, P. Ballo et al. - Bratislava : STU, 2015, p. 230-233. ISBN 978-80-227-4373-0.

2014:

- JERGEL, Matej - ŠIFFALOVIČ, Peter - VÉGSO, Karol - BENKOVIČOVÁ, Monika - VOJTKO, Andrej - MAJKOVÁ, Eva - LEE, H. - KU, C. - LIN, M. - JENG, U. **Reciprocal space mapping of silver nanoparticle array re-assembly and oxidation.** In *Acta Crystallographica A*, 2014, vol. 70, c745. (abstract)



- ŠIFFALOVIČ, Peter - JERGEL, Matej - BENKOVIČOVÁ, Monika - VOJTKO, Andrej - NÁDAŽDY, Vojtech - IVANČO, Ján - BODÍK, M. - DEMYDENKO, M. - MAJKOVÁ, Eva. **Towards new multifunctional coatings for organic photovoltaics.** In *Solar Energy Materials and Solar Cells*, 2014, vol. 125, p. 127-132.
  - BELLA, F. – GRIFFINI, G. – GEROSA, M. – TURRI, S. – BONGIOVANNI, R. **Performance and stability improvements for dye-sensitized solar cells in the presence of luminescent coatings.** In *Journal of Power Sources*, 2015, vol. 283, p. 195-203.
  - GRIFFINI, G. – BELLA, F. – NISIC, F. – DRAGONETTI, C. – ROBERTO, D. – LEVI, M. – BONGIOVANNI, R. – TURRI, S. **Multifunctional Luminescent Down-Shifting Fluoropolymer Coatings: A Straightforward Strategy to Improve the UV-Light Harvesting and Long-Term Outdoor Stability of Organic Dye-Sensitized Solar Cells.** In *Advanced Energy Materials*, 2014, vol. 5, 1401312.
  
- ŠIFFALOVIČ, Peter - VÉGSO, Karol - BENKOVIČOVÁ, Monika - JERGEL, Matej - VOJTKO, Andrej - HODAS, Martin - LUBY, Štefan - LEE, Hsin-Yi - KU, Man-Ling - JENG, U-Ser - SU, Chun-jen - MAJKOVÁ, Eva. **Reassembly and oxidation of a silver nanoparticle bilayer probed by in situ x-ray reciprocal space mapping.** In *Journal of Physical Chemistry C*, 2014, vol. 118, p. 7195-7201.
  - LIU, K. – LI, HY. – LU, Y. – WANG, RJ. – BEI, FL. – LU, LD. – HAN, QF. – WU, XD. **A completely controlled sphere-to-bilayer micellar transition: the molecular mechanism and application on the growth of nanosheets.** In *Soft Matter*, 2016, v. 12, p. 3703-3709.

### Conference contributions:

2016:

- VOJTKO, Andrej – ŠIFFALOVIČ, Peter – VEGSO, Karol – JERGEL, Matej – LUBY, Štefan – NÁDAŽDY, Vojtech – LEE, Hsin-Yi – KU, Ching-Shun – LIN, Man-Ling – JENG, U-Ser – SU, Chun-Jen - CESARIA, Maura – MAJKOVÁ, Eva. **GISAXS and GIWAXS study of P3HT:PCBM bulk heterojunction after UV nanosecond pulse laser irradiation.** In *New Trends in Solar Cells*, Bratislava, 2016.
  
- IVANČO, Ján – HALAHOVETS, Yuriy – VEGSO, Karol – KLAČKOVÁ, Ivana – KOTLÁR, Mário – VOJTKO, Andrej – MIČUŠÍK, Matej – JERGEL, Matej – MAJKOVÁ, Eva. **Cyclopean gauge factor of the strain-resistance transduction of indium oxide films.** *IOP Conference Series: Materials Science and Engineering*, 2016, vol. 108, 1, p. 012043.

2015:

- BENKOVIČOVÁ, Monika - KOTLÁR, Mário - VOJTKO, Andrej - JERGEL, Matej - ŠIFFALOVIČ, Peter - VÉGSO, Karol - LUBY, Štefan - MAJKOVÁ, Eva. **Synthesis of gold nanorods with different aspect ratio for organic photovoltaics.** In *APCOM 2015 : Proceedings of the 21st International Conference on Applied Physics of Condensed Matter*. Eds. J. Vajda, I. Jamnický ; rev. J. Sitek, P. Ballo et al. - Bratislava : STU, 2015, p. 230-233. ISBN 978-80-227-4373-0.

- VOJTKO, Andrej - BENKOVIČOVÁ, Monika - HALAHOVETS, Yuriy - JERGEL, Matej - KOTLÁR, Mário - KAISER, Michal - ŠIFFALOVÍČ, Peter - NÁDAŽDY, Vojtech - MAJKOVÁ, Eva. **P3HT:PCBM based organic solar cells: Structure optimization and improving external quantum efficiency by plasmonic nanoparticles incorporation.** In Nano-Structures for Optics and Photonics: Optical strategies for enhancing sensing, imaging, communication and energy conversion : Proceedings of the NATO Advanced Study Institute on Nano-Structures for Optics and Photonics. - Dordrecht : Springer, 2015, p. 561-563. ISBN 978-94-017-9142-7.  
- KHAN, M. S. – AL-SUTI, M. K. – MAHARAJA, J. – HAQUE, A. – AL-BALUSHI, R. – RAITHBY, P. R. **Conjugated poly-ynes and poly(metalla-ynes) incorporating thiophene-based spacers for solar cell (SC) applications.** In *Journal of Organometallic Chemistry*, 2016, vol. 812, p. 13-33.
- VOJTKO, Andrej - BENKOVIČOVÁ, Monika - NÁDAŽDY, Vojtech - KAISER, Michal - IVANČO, Ján - JERGEL, Matej - ŠIFFALOVÍČ, Peter - MAJKOVÁ, Eva. **Different plasmonic light trapping mechanisms in P3HT:PCBM organic solar cells with incorporated nanoparticles.** In APCOM 2015 : Proceedings of the 21st International Conference on Applied Physics of Condensed Matter. Eds. J. Vajda, I. Jamnický ; rev. J. Sitek, P. Ballo et al. - Bratislava : STU, 2015, p. 342-345. ISBN 978-80-227-4373-0.
- VOJTKO, Andrej - ŠIFFALOVÍČ, Peter - JERGEL, Matej - VÉGSO, Karol - NÁDAŽDY, Vojtech - LEE, H.-Y. - KU, Ch.-Sh. - LIN, M.-L. - JENG, U.-S. - SU, Ch.-J. - MAJKOVÁ, Eva. **Pulsed UV laser annealing of P3HT:PCBM blend for active layer of organic solar cells.** In Proceedings of the 3th International Conference on Advances in Electronic and Photonic Technologies, June 1-4, 2015, Štrbské Pleso, Slovakia : ADEPT 2015. Eds. D. Pudiš, I. Lettrichová, J. Kováč, jr. - Žilina : Univ. Žilina, 2015, p. 84-87. ISBN 978-80-554-1033-3

2014

- BENKOVIČOVÁ, Monika - KOTLÁR, Mário - KOTLÁR, Mário - JERGEL, Matej - ŠIFFALOVÍČ, Peter - VOJTKO, Andrej - VÉGSO, Karol - LUBY, Štefan - MAJKOVÁ, Eva. **Preparation of metallic nanorods for plasmonic applications by chemical way.** In Proceedings of the 20th International Conference on Applied Physics of Condensed Matter : APCOM 2014. Eds. J.Vajda, I.Jamnický. - Bratislava : FEI STU, 2014, p. 210-213.
- BODIK, M. - ŠIFFALOVÍČ, Peter - NÁDAŽDY, Vojtech - VOJTKO, Andrej - KAISER, Michal - VÉGSO, Karol - HODAS, Martin - JERGEL, Matej - MAJKOVÁ, Eva - ŠPITALSKÝ, Zdenko - OMASTOVÁ, Mária. **Modified langmuir-Schaefer method for large-scale deposition of graphene oxide layers in polymer solar cell research.** In graphene 2014 : International Conference & Exhibition : Toulouse, France, May 06-09, 2014 : poster book vol. 1. - Toulouse, France : Phantoms foundations, 2014.
- ŠIFFALOVÍČ, Peter - JERGEL, Matej - VOJTKO, Andrej - NÁDAŽDY, Vojtech - IVANČO, Ján - BODIK, M. - DEMYDENKO, M. - MAJKOVÁ, Eva. **O2B- Superhydrophobic nanoparticle coatings for polymer solar cells.** In Proceedings of the 1st International Symposium on Nanoparticles/ Nanomaterials and Applications (ISN2 A 2014) : Book of Abstracts. - Caparica : Proteomass Scientific Society, 2014, p. 127.

2013

- GMUCOVÁ, Katarína - NÁDAŽDY, Vojtech - VOJTKO, Andrej - KOTLÁR, Mário - MAJKOVÁ, Eva. **Investigation of ion diffusion towards plasmonic surfaces.** In Proceedings of the 19th International Conference on Applied Physics of Condensed Matter : APCOM 2013. Eds. J.Vajda, I.Jamnický. - Bratislava : Nakladateľstvo STU Bratislava, 2013, p. 229-232. ISBN 978-80-227-3956-6.
- GMUCOVÁ, Katarína - NÁDAŽDY, Vojtech - BENKOVIČOVÁ, Monika - VOJTKO, Andrej - KOTLÁR, Mário - WEIS, Martin Jr. - ŠATKA, A. - MAJKOVÁ, Eva. **Fractal dimension of nanoparticle modified surfaces.** In Proceedings of the 20th Conference of Slovak Physicists, September 2-5, 2013, Bratislava. - Bratislava : Slovak Physical Society, 2014, p. 41-42. ISBN 978-80-971450-2-6.
- MAJKOVÁ, Eva - VOJTKO, Andrej - JERGEL, Matej - NÁDAŽDY, Vojtech - BENKOVIČOVÁ, Monika - ŠIFFALOVICH, Peter - KOTLÁR, Mário. **Organic photovoltaic devices- promising alternative for renewable energy resources.** In Renewable Energy Sources 2013 : Proceedings of the 4th International Scientific Conference OZE 2013, May 21-23, Tatranské Matliare, Slovakia. - Bratislava : Slovak University of Technology, 2013, p. 15-17. ISBN 978-80-89402-64-9.
- VOJTKO, Andrej - BENKOVIČOVÁ, Monika - JERGEL, Matej - KOTLÁR, Mário - HALAHOVETS, Yuriy - ŠIFFALOVICH, Peter - NÁDAŽDY, Vojtech - MAJKOVÁ, Eva. **Application of plasmonic nanoparticles in organic photovoltaic structures.** In Proceedings of ADEPT : 1st International Conference on Advances in Electronic and Photonic Technologies. Eds. D. Pudiš et al. - Žilina : University of Žilina, 2013, p. 24-27. ISBN 978-80-554-0689-3.